

Detection of previously frozen poultry through plastic lidding film using portable visible spectral imaging (443–726 NM)

Anastasia Swanson ¹ and Aoife Gowen 

UCD School of Biosystems and Food Engineering, University College Dublin, Dublin 4, Ireland

ABSTRACT The objective of this study is to use a portable visible spectral imaging system (443–726 nm) to detect poultry thawed from frozen at the pixel level using multivariate analysis methods commonly used in machine learning (decision tree, logistic regression, linear discriminant analysis [LDA], k-nearest neighbors [KNN], support vector machines [SVM]). The selection of the most suitable method is based on the amount of data required to build an accurate model, computational speed, and the robustness of the model. The training set consists of pixel spectra from packages of chicken thighs without plastic lidding to evaluate the robustness of the models when implemented on the test set with and without plastic lidding. Data subsets were created by

randomly selecting 1, 5, 10, 20, and 50% of the pixel spectra of each sample for both the training and test data sets. The subsets of pixel spectra and the full training set were used to train the machine learning algorithms to evaluate how the amount of data influences computational time. Logistic regression was found to be the best algorithm for detecting poultry thawed from frozen with and without plastic lidding film. Although logistic regression and SVM both performed with the same high accuracy and sensitivity for all training subset sizes, the computational time needed to implement SVM makes it the less suitable algorithm for detecting poultry thawed from frozen with and without plastic lidding film.

Key words: portable spectral imaging, poultry, frozen-thawed, machine learning, multivariate analysis

2022 Poultry Science 101:101578

<https://doi.org/10.1016/j.psj.2021.101578>

INTRODUCTION

To meet consumer demands for fresh meat while benefiting from increased shelf life of frozen meat, retailers may be influenced to label products thawed from frozen as fresh meat. Although freezing can prolong shelf-life of poultry products, lipid and protein oxidation increase while water holding capacity and color stability decrease with each freeze-thaw cycle (Ali et al., 2015). Current authentication techniques (i.e., enzymatic, DNA based, spectroscopic, bio-imaging, sensory etc.) are time consuming, destructive, and rely on trained professionals (Ballin and Lametsch, 2008). Spectral imaging is proposed as an alternative method, which combines conventional imaging with spectroscopy to obtain spatial and chemical information about samples. Although there are many examples of using spectral imaging to detect thawed pork (Barbin et al., 2013; Ma et al., 2015; Cheng et al., 2018), applying spectral

imaging to detecting frozen-thawed poultry is a gap in the current literature (Antequera et al., 2021). However, recent point-spectroscopic attempts have been made to detect frozen-thawed poultry in the using Fourier transform infrared (FTIR) spectroscopy (Grunert et al., 2016) and nuclear magnetic resonance (NMR) spectroscopy (Soglia et al., 2019). Using an artificial neural network, FTIR spectroscopy was successful in detecting frozen-thawed chicken. The results indicated that changes to the protein structure had occurred during freezing. Soglia et al. (2019) also found significant changes in amino acid composition and increased protein oxidation following freezing using NMR spectroscopy. However, the methods used by both Grunert et al. (2016) and Soglia et al. (2019) require extensive and destructive sample preparation. In a previous study comparing Vis-NIR and NIR spectral imaging, it was possible to discriminate between unpackaged fresh and thawed chicken thighs with data obtained from a laboratory based Vis-NIR spectral imaging system (400–1,000 nm) with halogen illumination using a partial least squares discriminant analysis (PLS-DA) model of individual chicken thighs (Falkovskaya et al., 2019). Successful detection of thawed poultry could be accomplished using pixel level models, resulting in a correct classification rate of 88.2% in the test set (LV = 10,

© 2021 The Authors. Published by Elsevier Inc. on behalf of Poultry Science Association Inc. This is an open access article under the CC BY-NC-ND license (<http://creativecommons.org/licenses/by-nc-nd/4.0/>).

Received September 17, 2020.

Accepted November 2, 2021.

¹Corresponding author: anastasia.falkovskaya@ucdconnect.ie

sensitivity = 92.1%, specificity = 84.2%). Wavelengths determined to be important for discrimination by the regression coefficients of the PLS-DA model include: 500, 575, 595, and 620 nm. These wavelengths are within the range of wavelengths associated with myoglobin and its redox forms which are responsible for the red color in tissue (Tang et al., 2004). Because these wavelengths are in the visible light range, this opens the possibility of using visible spectral imaging with LED illumination. Using LED illumination may be more attractive to food processors and retailers, as it is more efficient, widely available, and produces less heat than traditional halogen lighting required for NIR spectral imaging.

For spectral imaging to work as an on-site solution to detect poultry products thawed from frozen, product classification should occur without the need remove products from the packaging. However, poultry products are generally sold in plastic tray packaging covered by a transparent plastic lidding film made of polyethylene terephthalate (PET) or in combination with either polyethylene (PET/PE) or polypropylene (PET/PP). Previously, spectral imaging in the Vis-NIR range has been successfully used to evaluate quality of mushrooms through PET packaging film (Taghizadeh et al., 2010), detecting thawed from frozen cod through polyamide/PE vacuum packaging (Washburn et al., 2017), monitoring spinach shelf-life through 3 different kinds of PP (Lara et al., 2013), and detecting *Escherichia coli* contamination in packaged fresh spinach through low-density PE packaging (Siripatrawan et al., 2011). Packaging films influence light scattering of Vis-NIR spectral images based on the relative positions between the light source, sample, and detector. Using various spectral pre-treatment techniques, it is possible to reduce the effect of light scattering caused by multiple reflections on the air-film-air interface and artifacts from light reflected from the film to the detector (Gowen et al., 2010). Pre-treatment of spectra by standard normal variate (SNV) followed by first order Savitzky–Golay was shown to

reduce variability introduced by scattering effects of polymer films (Gowen et al., 2010).

Recent advances in technology have allowed for the development of portable/handheld spectral imaging systems (Behmann et al., 2018; Kruglikov et al., 2019; Barreto et al., 2020), which would allow for product classification without the need to bring samples to a laboratory setting. In this context, the aim of this study is to evaluate the application of portable spectral imaging to detecting thawed poultry with and without plastic lidding films.

METHODS

Poultry Samples

Ten packages of Class A chicken thighs with skin on (1,203 g each) from cereal fed chickens were acquired from a local supermarket. All packages were selected to have the same ‘use-by’ date, to control for the effects of color changes due to storage time. Treatment samples were frozen at -18°C for 48 h, after which they were moved to 4°C for a further 24 h. Meanwhile, control samples were kept at 4°C for the same total duration of time (72 h). Each package contains between 7 and 9 individual chicken thighs, resulting in a total of 84 samples. Packs were removed from 4°C directly before imaging. The training set consists of 3 control ($n_{\text{samples}} = 25$) and 3 thawed ($n_{\text{samples}} = 25$) packages imaged with the plastic lidding removed. The test set consists of 2 control ($n_{\text{samples}} = 17$) and 2 thawed ($n_{\text{samples}} = 17$) packages first imaged with the plastic lidding, and then with the plastic lidding removed (Figure 1). Poultry is highly perishable, with significant color changes occurring due to the oxidation of myoglobin (Suman and Joseph, 2013). If the fresh poultry was imaged at 0 h and the thawed poultry was imaged at 72 h, the model may reflect more the effects of aging than the effects of freezing. Therefore, both treatments were imaged at the same time-point.

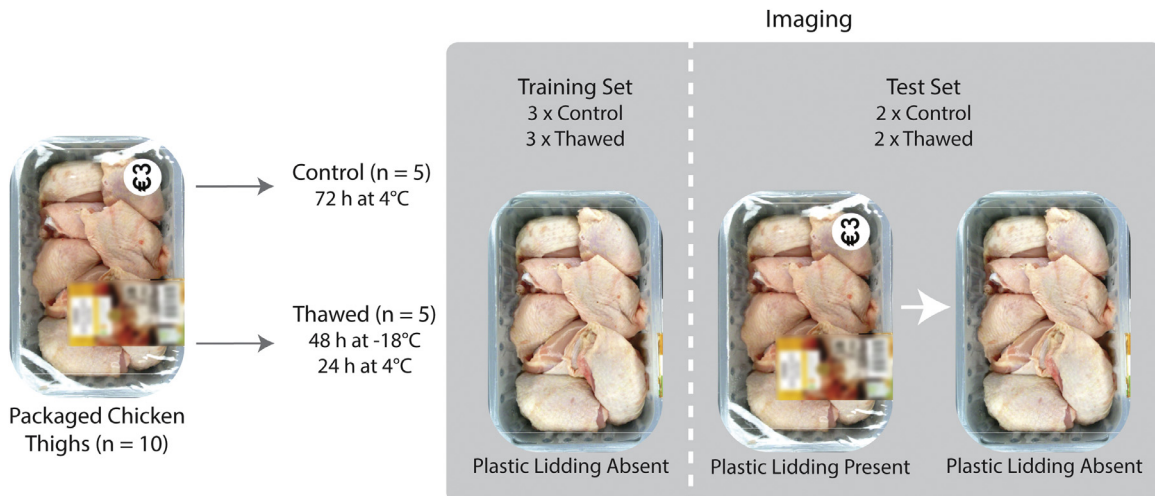


Figure 1. Schematic showing experimental setup and number of images (n). Each package contains 7–9 individual samples. The samples shown in the figure is a control package, depicting that all samples were kept in plastic lidding covered packages prior to imaging. Training set samples were imaged with the plastic lidding removed. Test set samples were imaged with the plastic lidding present and absent.

Spectral Imaging System and Software

Spectral images were acquired using a portable Specim IQ camera system (Specim, Spectral Imaging Ltd., Oulu, Finland) using white LED ring light illumination (Venus V29C, Guangdong Nanguang Photo&Video Systems Co., Ltd, Shantou, Guangdong, China) around the lens of the camera. The Specim IQ is a pushbroom system operating from 400 to 1,000 nm with a spectral resolution of 7 nm. Resulting spectral images were 512 rows \times 512 columns \times 204 spectral bands. The spectral camera was positioned directly above the sample at a height of 46 cm, resulting in a pixel size of approximately 0.49 mm \times 0.49 mm. Alongside the spectral camera, an RGB camera within the Specim IQ captures RGB images of 512 \times 512 pixels. All samples were placed on a black paper surface for imaging.

The software used to acquire spectral images was Specim IQ Studio (Specim Ltd., Oulu, Finland). All data analysis was completed using MATLAB R2018b (MathWorks, MA) using functions from the Statistics and Machine Learning Toolbox and the Image Processing Toolbox.

Data Pretreatment

All images were first pre-treated by cutting the spectral range to 443 to 726 nm, to match the spectral range of the white LED illumination. Next, spectra were corrected using SNV and a Savitzky–Golay smoothing filter (13-point window size, second order, first derivative). This order of pretreatments was selected as it has been shown to reduce variability introduced by scattering effects of polymer films (Gowen et al., 2010).

Image Segmentation

Spectral images were manually cropped to exclude the background. In images with the plastic lidding film present, images were manually cropped to exclude 2 sticker labels on top of the lidding film. Pixels oversaturated due glare from the plastic tray were masked out using a manual threshold. Next, images were masked by using Otsu’s method of automatic threshold selection on the score image of the first principal component (PC1) to segment the meat from the plastic tray (Otsu, 1979).

Multivariate Analysis Methods

To investigate the performance and robustness of portable spectral imaging for the detection of poultry thawed from frozen, 5 of the most popular machine learning algorithms (decision tree, logistic regression, linear discriminant analysis [LDA], k-nearest neighbors [KNN], support vector machines [SVM]) are tested in this work. The selection of the algorithm best suited to this problem is based on the amount of data required to build an accurate model, computational speed, and the robustness of the model. Each of the machine learning

algorithms evaluated has their own advantages and disadvantages (i.e., simplicity, ability to handle nonlinear classification, ability to handle outliers, etc.), as follows:

Decision Tree Decision trees have a “tree” structure, where nodes represent simple tests on the individual features, branches are the outcomes of the tests at that node, and the terminal nodes are the class labels (James et al., 2013). Decision trees separate the input space so that each input feature (e.g., a vector of reflectance or absorbance at different wavelength bands) is evaluated individually (e.g., using a threshold to partition the feature space) in a recursive way to ultimately predict which class the observation belongs to (Kotsiantis, 2013). Nodes are then ordered in a hierarchical way, based on criterion such as Gini’s diversity index to measure which node best divides the input into classes (Pal and Mather, 2003; Kotsiantis, 2013). An advantage of decision trees is that they are capable of dealing with nonlinear data, do not rely on any data distribution assumptions, and are computationally fast (Pal and Mather, 2003; Zulhaidi et al., 2007). Although decision trees have the advantage of being simple to use and intuitive to understand, they are generally not as robust or accurate as other models (James et al., 2013). For data sets with high dimensional feature spaces with high correlation between features (e.g., spectral data), classification accuracy could benefit from models that simultaneously consider multiple features rather than sequential testing (Pal and Mather, 2003). Further, errors can accumulate through the tree and affect prediction accuracy due to the hierarchical structure of decision trees (Safavian and Landgrebe, 1991).

Logistic Regression Logistic regression is a commonly used machine learning technique for binary classification problems. Logistic regression fits a sigmoid function to the input features using maximum likelihood estimation and then creates a linear decision boundary between classes to predict the probability of which class an observation belongs to (Hastie et al., 2009). An advantage is that it is simple to use and fast to implement. However, a limitation is that logistic regression works best when there is a linear relationship between the input features and target variables (James et al., 2013).

LDA LDA reduces data dimensionality in a way that maximizes separability between classes while minimizing within class scatter, so that a linear decision boundary can be used to predict which class observations belong to (Balakrishnama, 1998). Unlike logistic regression, LDA assumes that the input data has a Gaussian distribution and is homoscedastic, which allows the model to estimate with lower variance (Hastie et al., 2009). However, the assumptions make LDA less robust to outliers than logistic regression and when the Gaussian assumptions are not met, logistic regression performs better than LDA (James et al., 2013).

KNN For classification problems, the KNN algorithm assumes that data clustered close together belongs to one target class. For each input data point, the distance between the point and all other points is calculated and

sorted by the smallest distance, then the target class is predicted by the mode target class of the chosen number of neighbors (k). This method directly predicts the target class of the data without the need to first build a model (Dreiseitl and Ohno-Machado, 2002). The main disadvantage of KNN is that it becomes slow as the amount of data increases because all distances between points must be calculated.

SVM SVM build optimal separating hyperplanes between classes (James et al., 2013). The optimal hyperplane is found by calculating the distance between the points closest to the hyperplane (support vectors) of both classes, and maximizing that distance (margin) from the hyperplane (Cortes and Vapnik, 1995). SVM can be used for both linear and non-linear relationships between the input features and target variables, by mapping nonlinear features to a higher dimension feature space (Dreiseitl and Ohno-Machado, 2002). Unlike logistic regression, no probability is given of which target class an observation belongs to (Dreiseitl and Ohno-Machado, 2002).

Data Analysis

Mean reflectance spectra were calculated from the test set by selecting pixels in a region of interest (**ROI**) containing 3 chicken thighs unobstructed by labels per package with plastic lidding present. The corresponding ROI was selected from samples without plastic lidding to calculate their mean. To compare mean spectra of tissue types, ROI's were manually selected from the test set of control samples without plastic lidding representative of skin, meat, joints, and fat. To compare the effects of thawing on different tissue types, ROI's were manually selected from the test set of thawed samples without plastic lidding representative of skin, meat, and joints. Fat could not be compared between control and thawed samples as not enough fat tissue was present in thawed samples. Next, data subsets were created by randomly selecting 1, 5, 10, 20, and 50% of the pixel spectra of each sample for both the training ($n_{1\%} = 7,017$, $n_{5\%} = 35,096$, $n_{10\%} = 70,194$, $n_{20\%} = 140,392$, $n_{50\%} = 350,984$, $n_{100\%} = 701,973$) and test data sets ($n_{1\%} = 3,408$, $n_{5\%} = 17,047$, $n_{10\%} = 34,096$, $n_{20\%} = 68,194$, $n_{50\%} = 170,489$, $n_{100\%} = 340,981$). The subsets of pixel spectra and the full training set were used to train five different machine learning algorithms: decision tree, logistic regression, LDA, KNN, and SVM (Table 1). Working at the pixel-level allows for more variation within samples to be represented, capturing all classes within a sample (e.g., skin, meat, fat, bone). The computational time taken to train each model was recorded, and each model was validated by using hold-out validation on 25% of the training set data to obtain training set accuracy. The models were then applied to the test subsets and full test sets with and without plastic lidding present, recording the accuracy, sensitivity, specificity, and computation time. Sensitivity refers to the ability of the model to correctly detect a thawed sample

Table 1. Chosen parameter details of models used from the Statistics and Machine Learning Toolbox (MathWorks, MA).

Model	Parameters
Decision tree	Preset name: Fine Tree Maximum number of splits: 100 Split criterion: Gini's diversity index
Logistic regression	Preset name: Logistic Regression
LDA	Preset name: Linear Discriminant Covariance structure: Full
KNN	Preset name: Fine KNN Number of neighbors: 3 Distance metric: Euclidian Distance weight: Equal
SVM	Preset name: Linear SVM Kernel function: Linear Kernel scale: Automatic Box constraint level: 1

Abbreviations: KNN, k-nearest neighbors; LDA, linear discriminant analysis; SVM, support vector machines.

(Equation 1), whereas specificity refers to correctly detecting control samples (Equation 2; Altman and Bland, 1994):

$$\text{Sensitivity} = \frac{\text{true positives}}{\text{true positives} + \text{false negatives}} \quad (1)$$

$$\text{Specificity} = \frac{\text{true negatives}}{\text{true negatives} + \text{false positives}} \quad (2)$$

True positive refers to the number of correctly predicted thawed samples and *true negatives* refer to the number of correctly predicted control samples. *False negatives* are samples incorrectly predicted as control and *false positives* are samples incorrectly predicted as thawed. Finally, the models were used to create classification maps to visually assess the differences between the model predictions.

RESULTS AND DISCUSSION

Mean reflectance spectra of control and thawed poultry samples in the test set are visually most noticeably different between the wavelength range of 450 to 625 nm for packages with and without plastic lidding present (Figure 2). Samples are made up of several tissue components (e.g., skin, meat, joints, and fat), each with their own spectral signature (Figure 3). The samples are not only heterogeneous, but each package contains differing proportions of each tissue type. Qualitative differences in spectra appear between 450 and 625 nm when the same tissue types are compared, suggesting color, chemical, and physical changes in all tissues (Figure 4). Wavelength bands in this range are associated with myoglobin and its redox forms, which are responsible for the red color in tissue (Liu et al., 2004; Tang et al., 2004). As meat ages, lipid oxidation produces aldehydes that move into the endoplasm of muscle cells, and adduct myoglobin in a way that increases myoglobin oxidation and changes meat color (Faustman et al., 2010; Jeong et al., 2011; Suman and Joseph, 2013).

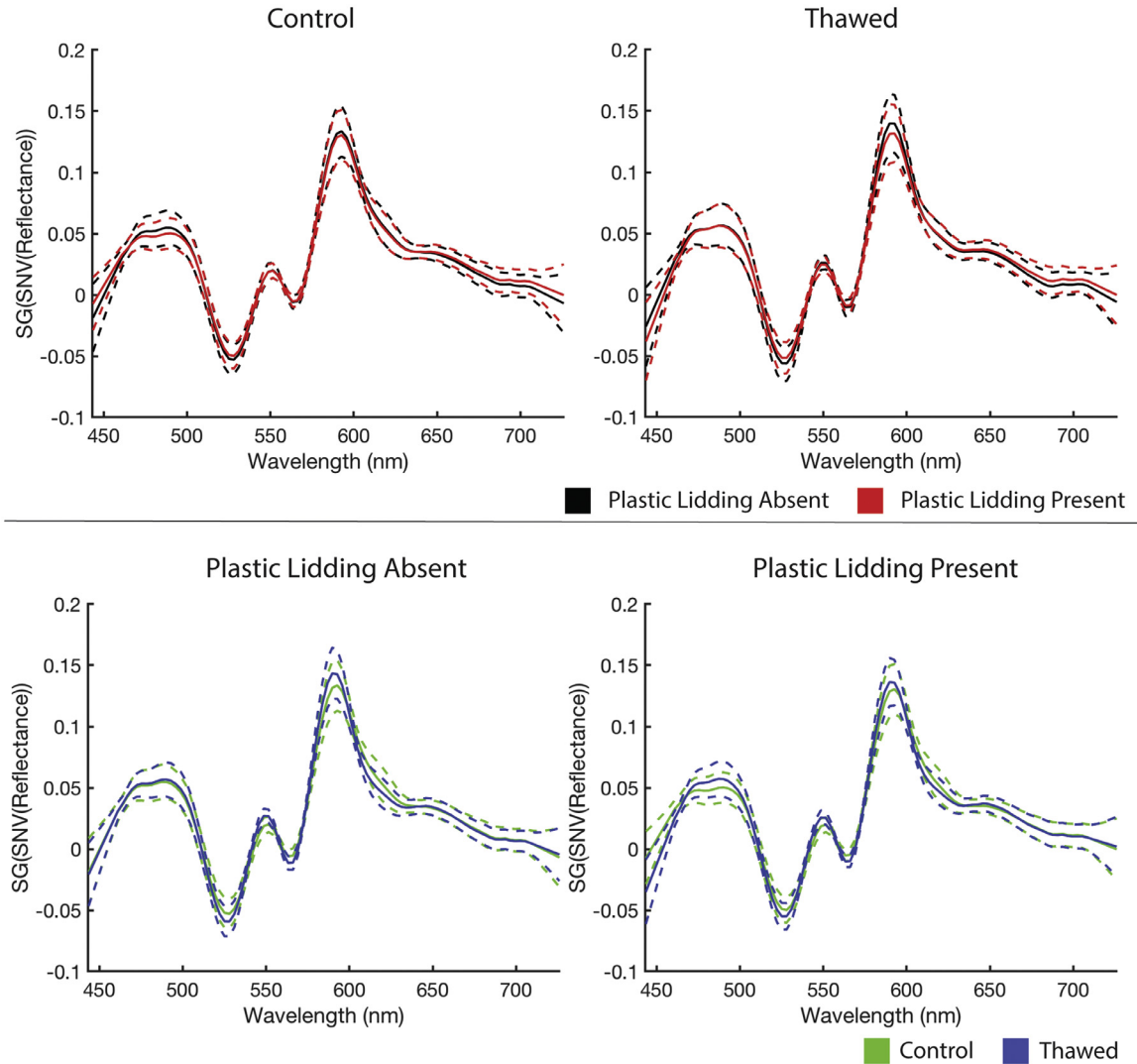


Figure 2. Mean reflectance (± 1 SD) spectra of control ($n_{\text{image}} = 2$) and thawed from frozen ($n_{\text{image}} = 2$) packaged chicken thighs in the test set with plastic lidding absent and present.

Although freezing meat is considered to be an effective method for preserving meat, initiation of primary lipid oxidation continues during freezing and leads to

accelerated lipid oxidation during thawing (Jeong et al., 2011; Leygonie et al., 2012). In experiments that measured lipid oxidation by measuring thiobarbituric acid reactive substances (TBARS), thawed beef and pork meat samples had higher levels of lipid oxidation than control samples of the same age (Hansen et al., 2004; Vieira et al., 2009). Increased lipid oxidation of thawed samples that induces increased myoglobin oxidation to oxymyoglobin could be responsible for the change in color of the thawed chicken samples in this work. As seen in RGB images, some thawed samples appear to have more red spotting on the skin surface, indicative of increased oxymyoglobin presence (Figure 5). However, these color changes are not obvious or intuitive to interpret by human inspection as symptomatic of thawed meat.

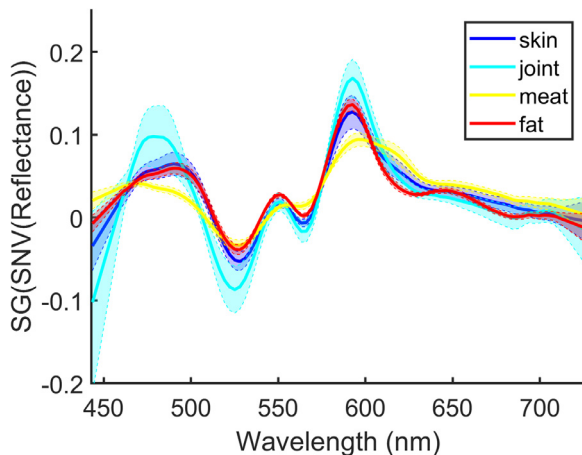


Figure 3. Mean spectral signatures (± 1 SD) of tissue types of a control sample ($n_{\text{sample}} = 1$) in the test set without plastic lidding. Spectra were pretreated by standard normal variate (SNV) preprocessing followed by Savitzky Golay (SG) smoothing (13-point window size, second order, first derivative).

Decision Tree

The decision tree model performed with the lowest accuracy in the training set, reaching a maximum of 82% accuracy using the full training set. When applied to the test set without plastic lidding, the model accuracy decreased to 80% (sensitivity = 77%,

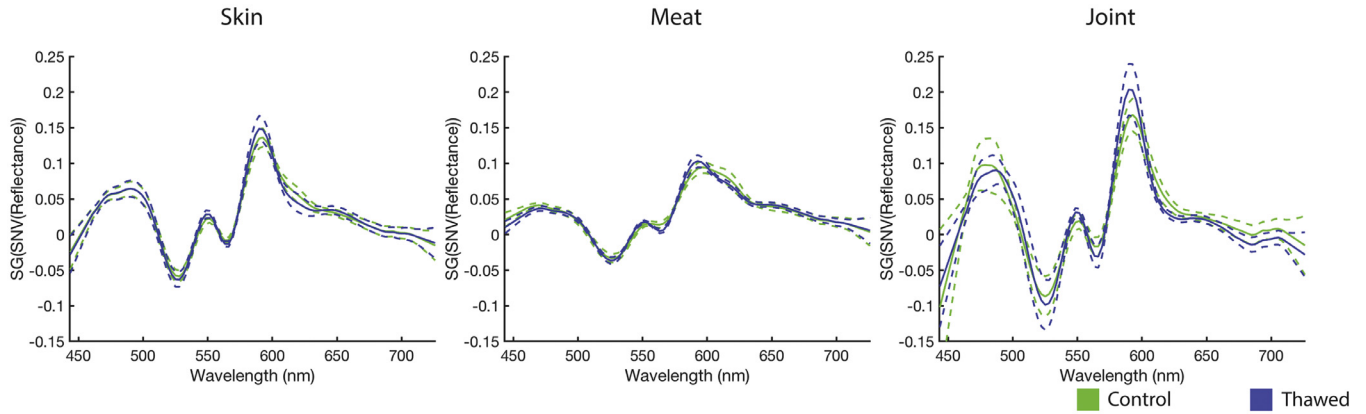


Figure 4. Mean reflectance (± 1 SD) spectra of control ($n_{\text{image}} = 2$) and thawed from frozen ($n = 2$) packaged chicken thighs in the test set without plastic lidding, grouped by tissue type.

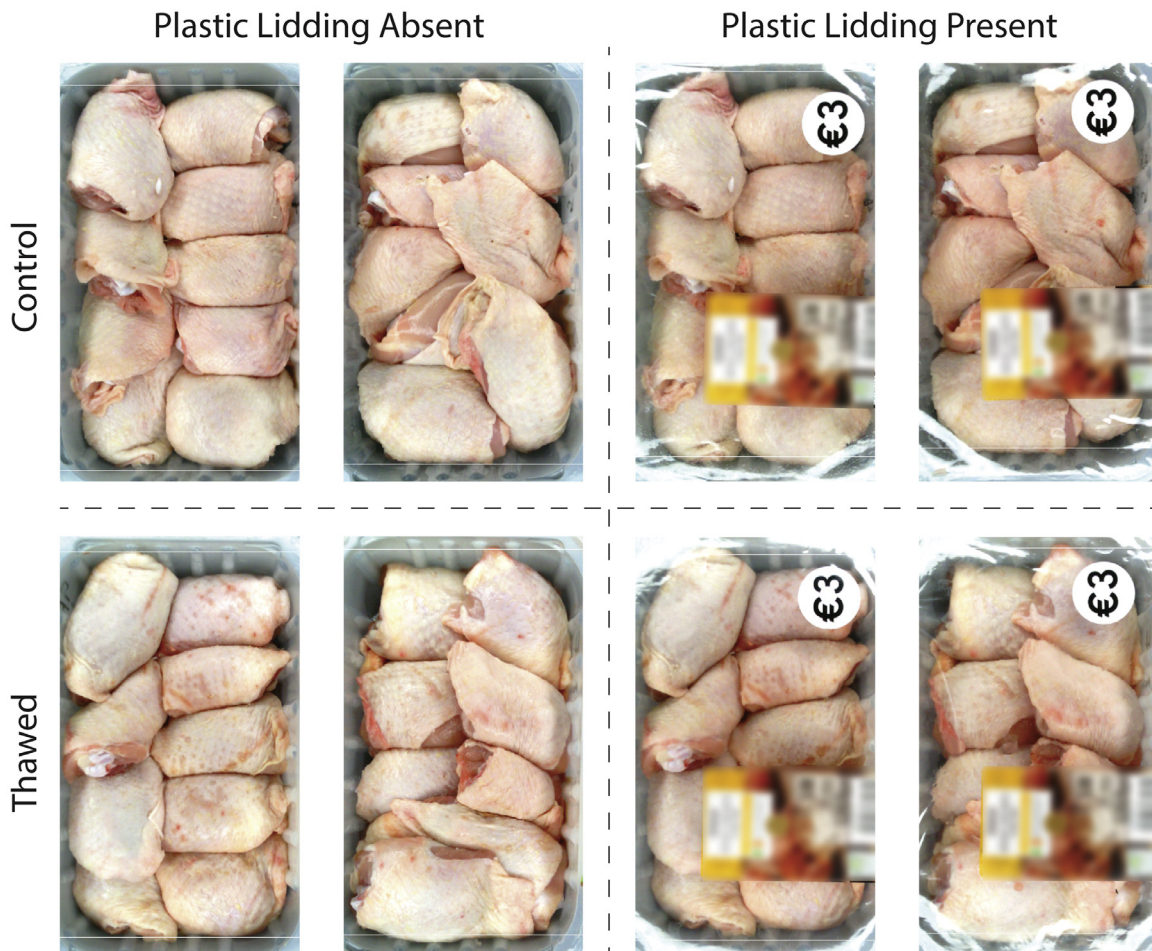


Figure 5. RGB images of packaged chicken thighs in the test set ($n_{\text{image}} = 4$) with plastic lidding absent and present.

specificity = 82%). Further, when the model was applied to the same test set with plastic lidding, accuracy again decreased to 77% (sensitivity = 81%, specificity = 74%). The amount of data used for training did not strongly influence accuracy in the training or test set (Figure 6). Although the full decision tree model was very fast to train ($t_{\text{training}} = 56.75$ s) and the fastest of all tested models to implement ($t_{\text{test (avg)}} = 0.67$ s), it was not as robust or accurate as other models. The full decision tree model ranks the third best model for accuracy (Table 2) and the first best for computational time (Table 2).

Logistic Regression

The logistic regression model performed with a maximum accuracy of 89% in the full training set. The amount of data used for training did not considerably affect the accuracy rates, with training set accuracy remaining between 87 and 89% for all training data subsets. The full model reached accuracy of 87% (sensitivity = 83%, specificity = 91%) when applied to the test set without plastic lidding, and remained unchanged at 87% (sensitivity = 83%,

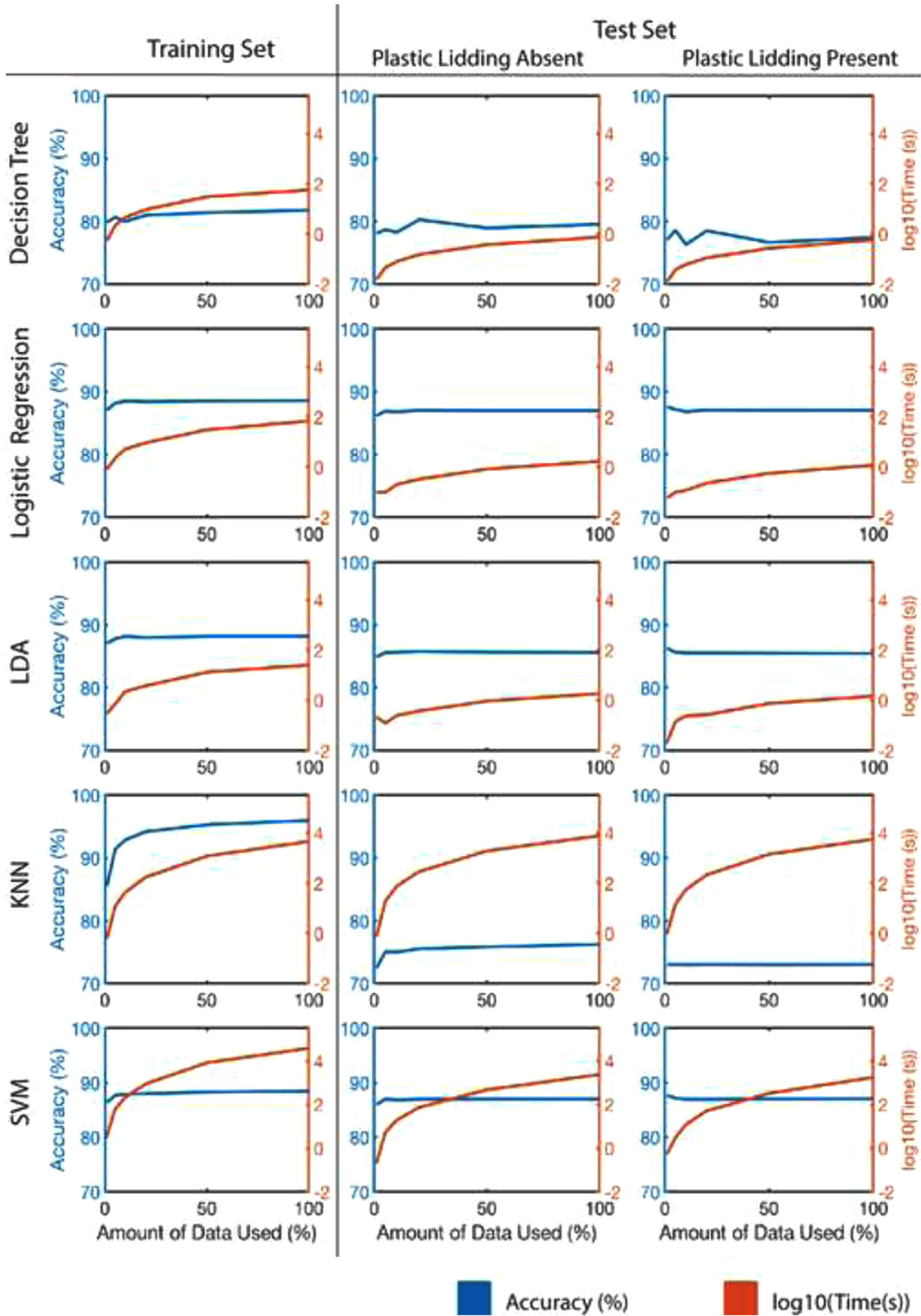


Figure 6. Comparison of machine learning algorithms on accuracy (%) and computational time (log₁₀(s)) of models trained using 1, 5, 10, 20, 50, and 100% of training pixel spectra.

specificity = 91%) when applied to the plastic covered test set. Accuracy remained between 86 and 87% for both test sets at all subset sizes, indicating the model is robust enough to maintain accuracy with plastic lidding light scattering. For the smallest training and test

subsets (1% of spectra), logistic regression ranks as the first most accurate model (Table 2). For the full model, logistic regression and SVM are equally ranked as the first most accurate model (Table 2). The full logistic regression model was fast to train ($t_{\text{training}} = 68.43$ s)

Table 2. Machine learning algorithms ranked by best mean computational time, accuracy, sensitivity, and specificity on both test sets.

Ranking	Time	Accuracy	Sensitivity	Specificity
1	Decision tree	Logistic regression; SVM	Logistic regression; SVM	LDA
2	Logistic regression	LDA	LDA	Logistic regression; SVM
3	LDA	Decision tree	KNN	KNN
4	SVM	KNN		Decision tree
5	KNN			

Abbreviations: KNN, k-nearest neighbors; LDA, linear discriminant analysis; SVM, support vector machines.

and implement ($t_{\text{test (avg)}} = 1.45$ s). Overall, the full logistic regression model ranks as the second best model for computational time (Table 2).

LDA

In the full training set, the LDA model performed with a maximum accuracy of 88%. Like logistic regression, the amount of data used did not have a considerable affect the accuracy rates, with the smallest subset (1% of spectra) performing with 87% accuracy in the training set. The full model reached accuracy of 86% (sensitivity = 79%, specificity = 92%) when applied to the test set without plastic lidding, and remained unchanged at 86% (sensitivity = 80%, specificity = 91%) when applied to the plastic covered test set. When applied to the test subsets, accuracy remained between 85-86% for all testing subsets for samples with and without plastic lidding, indicating high model robustness. For the full model testing set accuracy, LDA ranks second behind logistic regression and SVM (Table 2). The model was also fast to ($t_{\text{training}} = 25.10$ s) and implement ($t_{\text{test (avg)}} = 1.64$ s), ranking third for computational time (Table 2). However, computational time to implement the full LDA model was only a fraction of a second slower than logistic regression.

KNN

The KNN algorithm accuracy improved in the training set as the data subset included more of the data, from 86% when 1% of the data was included to 96% when the full training set was used. However, accuracy was the lowest of all algorithms tested in both test sets, ranking KNN last for model accuracy (Table 2). The maximum accuracy achieved when applied to the test set without plastic lidding was 76% (sensitivity = 68%, specificity = 84%). When the model was applied to the same test set with plastic lidding, accuracy again decreased to 73% (sensitivity = 70%, specificity = 79%). This is likely due to overfitting, as the accuracy of the training set was higher than the test set accuracy. The KNN algorithm was also computationally expensive, taking a long time to train ($t_{\text{training}} = 4,567.90$ s) and implement ($t_{\text{test (avg)}} = 6,705.12$ s) for the full model, ranking KNN as the fourth for computational time (Table 2). This algorithm was the least suited to discriminating between fresh and thawed poultry, due to its low accuracy and long computational time.

SVM

The SVM model performed with accuracy as high as logistic regression for training and test sets, at 87 to 88%. The full model reached accuracy of 87% (sensitivity = 83%, specificity = 91%) when applied to the test set without plastic lidding, and remained unchanged at 86% (sensitivity = 83%, specificity = 91%) when applied to the plastic covered test set. Accuracy was not affected by the amount of data used and the model was robust enough to not be affected by plastic lidding. For the full model testing set accuracy, SVM ranks first alongside logistic regression (Table 2). Although SVM was the most computationally expensive model to train ($t_{\text{training}} = 38,480.00$ s), it was less computationally expensive to implement ($t_{\text{test (avg)}} = 2,084.60$ s) than KNN, ranking SVM as fourth for computational time (Table 2).

Optimal Method

Despite considerable heterogeneity in tissue spectral response, the developed model can detect previously frozen. Logistic regression is proposed as the optimal method for detecting poultry thawed from frozen. Despite considerable heterogeneity in tissue spectral response, the developed model can detect thawed poultry with high accuracy and sensitivity with short computational time. Wavelengths corresponding to the highest

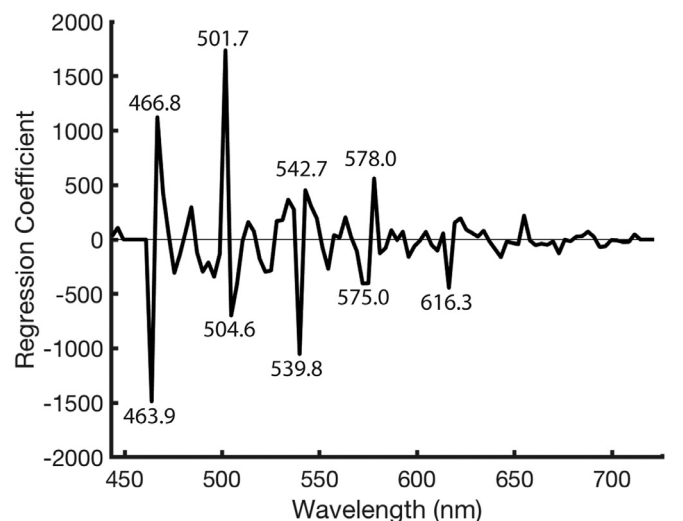


Figure 7. Regression coefficients of the full logistic regression model.

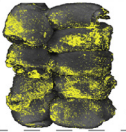
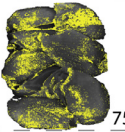

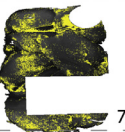
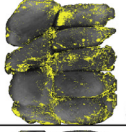
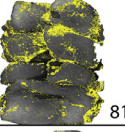
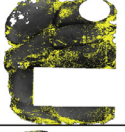
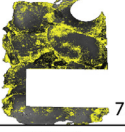
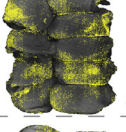
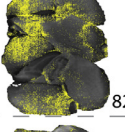


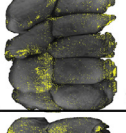
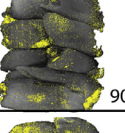
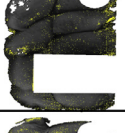
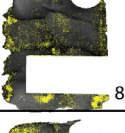
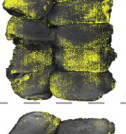
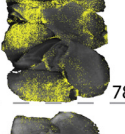
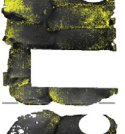
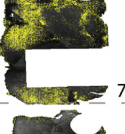
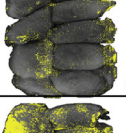
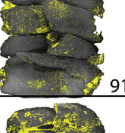
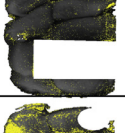
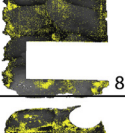
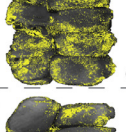
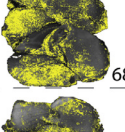
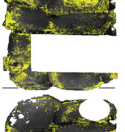
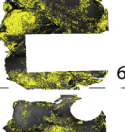
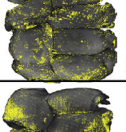
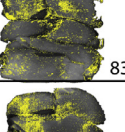
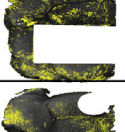
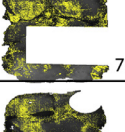
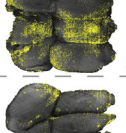
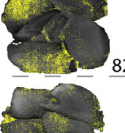
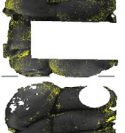

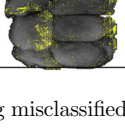
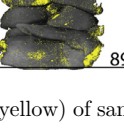
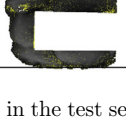
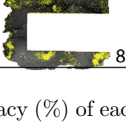
	Plastic Lidding Absent		Plastic Lidding Present		Average Accuracy	
Decision Tree	Control	 78%	 75%	 83%	 78%	78%
	Thawed	 83%	 81%	 78%	 70%	
Logistic Regression	Control	 83%	 82%	 87%	 79%	87%
	Thawed	 93%	 90%	 94%	 87%	
LDA	Control	 80%	 78%	 85%	 74%	85%
	Thawed	 94%	 91%	 95%	 87%	
KNN	Control	 69%	 68%	 73%	 66%	75%
	Thawed	 85%	 83%	 82%	 76%	
SVM	Control	 84%	 82%	 88%	 79%	87%
	Thawed	 93%	 89%	 95%	 87%	

Figure 8. Maps showing misclassified pixels (yellow) of samples in the test set, accuracy (%) of each algorithm on individual packages and the average accuracy (%).

absolute values of the logistic regression model vector of coefficients (β) were identified as the most important for classification: 463.9, 466.8, 501.7, 504.6, 539.8, 542.7, 575.0, 578.0, 616.3 nm (Figure 7). In previous experiments using nonportable spectral imaging, regression coefficients from a PLS-DA model indicated 500, 575, 595, and 620 nm as the most important for detecting thawed poultry (Falkovskaya et al., 2019). Differences between the sets of regression vectors could be a result of smoothing during spectral pre-treatments, resulting in slight variations in coefficient values at wavelengths. In current literature, there is no consensus on particularly which wavelengths correspond to peaks of

myoglobin redox forms. For example, Tang et al. (2004) attribute the peaks at 503 nm to metmyoglobin, 557 nm to deoxymyoglobin, and 582 nm to oxymyoglobin using prepared stock solutions representative of meat producing species. Meanwhile, Liu et al. (2004) attribute peaks at 445 nm to deoxymyoglobin, 485 nm to metmyoglobin, 560 nm to oxymyoglobin, and 635 nm to sulfmyoglobin in thawed skinless chicken breast samples. However, the wavelengths indicated as important by this study are within the range of wavelengths associated with myoglobin and its redox forms which are responsible for the red color in tissue (Liu et al., 2004; Tang et al., 2004).

Maps of Misclassified Pixels

For all tested models, misclassification of pixels is more evident in control than thawed samples (Figure 8). If the models are classifying based on color changes due to myoglobin oxidation, as is strongly suggested by inspection of the logistic regression coefficients, this could be a result of variation of lipid oxidation rates over the sample surface as the meat naturally ages in control samples. In contrast, the myoglobin in thawed samples has already oxidized resulting in a more stable color and therefore more accurate prediction rate. The same trend was observed when the models were applied to the training set samples, as shown in the supplementary material.

CONCLUSIONS

Poultry thawed from frozen can be detected using portable spectral imaging in the visible wavelength range (443–720 nm) using multivariate analysis methods commonly used in machine learning. Of the 5 methods tested (decision tree, logistic regression, LDA, KNN, SVM), logistic regression was found to be the most suitable algorithm for detecting poultry thawed from frozen with and without plastic lidding film covering samples. The full logistic regression model had the highest accuracy (87%) and sensitivity (83%) when applied to the test set without plastic lidding and remained unchanged when applied to the plastic covered test set, indicating the model is robust enough to handle plastic lidding light scattering. Further, the amount of data used for training did not considerably affect the prediction results. Although logistic regression and SVM both performed with the same high accuracy and sensitivity, the computational time needed to implement SVM makes it less suitable to detecting thawed poultry. LDA is also a reasonable option, as it results in higher specificity and only slightly lower accuracy and sensitivity in test sets while remaining faster than SVM to implement. Although decision trees are quick to implement, they resulted in low classification accuracy and were less robust to the lidding films. Finally, the KNN algorithm resulted in the lowest accuracy in the test sets and was very time consuming to train and implement.

ACKNOWLEDGMENTS

Funding for this project was provided by the Department of Food Agriculture and the Marine (Grant No. 17/F/275), under the Food Institutional Research Measure (FIRM).

DISCLOSURES

The authors declare no conflict of interest.

SUPPLEMENTARY MATERIALS

Supplementary material associated with this article can be found in the online version at [doi:10.1016/j.psj.2021.101578](https://doi.org/10.1016/j.psj.2021.101578).

REFERENCES

- Ali, S., W. Zhang, N. Rajput, M. A. Khan, C.-B. Li, and G.-H. Zhou. 2015. Effect of multiple freeze - thaw cycles on the quality of chicken breast meat. *Food Chem.* 173:808–814.
- Altman, D. G., and J. M. Bland. 1994. Statistics notes: diagnostic tests 1: sensitivity and specificity. *Br. Med. J.* 308:1552.
- Antequera, T., D. Caballero, S. Grassi, B. Uttaro, and T. Perez-Palacios. 2021. Evaluation of fresh meat quality by hyperspectral imaging (HSI), nuclear magnetic resonance (NMR) and magnetic resonance imaging (MRI): a review. *Meat Sci.* 172:108340.
- Balakrishnama, S. 1998. Linear discriminant analysis - a brief tutorial. *Institute for Signal and information.* Processing 18(1998):1–8.
- Ballin, N. Z., and R. Lametsch. 2008. Analytical methods for authentication of fresh vs. thawed meat - a review. *Meat Sci.* 80:151–158.
- Barbin, D. F., D. W. Sun, and C. Su. 2013. NIR hyperspectral imaging as non-destructive evaluation tool for the recognition of fresh and frozen-thawed porcine longissimus dorsi muscles. *Innov. Food Sci. Emerg. Technol.* 18:226–236.
- Barreto, A., S. Paulus, M. Varrelmann, and A. K. Mahlein. 2020. Hyperspectral imaging of symptoms induced by *Rhizoctonia solani* in sugar beet: comparison of input data and different machine learning algorithms. *J. Plant Dis. Prot.* 127:441–451.
- Behmann, J., K. Acebron, D. Emin, S. Bennertz, S. Matsubara, S. Thomas, D. Bohnenkamp, M. Kuska, J. Jussila, H. Salo, A.-K. Mahlein, and U. Rascher. 2018. Specim IQ: evaluation of a new, miniaturized handheld hyperspectral camera and its application for plant phenotyping and disease detection. *Sensors* 18:441.
- Cheng, W., D. W. Sun, H. Pu, and Q. Wei. 2018. Characterization of myofibrils cold structural deformation degrees of frozen pork using hyperspectral imaging coupled with spectral angle mapping algorithm. *Food Chem.* 239:1001–1008.
- Cortes, C., and V. Vapnik. 1995. Support-Vector Networks. Kluwer Academic Publishers, Dordrecht, the Netherlands.
- Dreiseitl, S., and L. Ohno-Machado. 2002. Logistic regression and artificial neural network classification models: a methodology review. *J. Biomed. Inform.* 35:352–359.
- Falkovskaya, A., A. Herrero-Langreo, and A. Gowen. 2019. Comparison of Vis-Nir (400-1,000 Nm) and Nir (978-1,678 Nm) hyperspectral imaging for discrimination between fresh and previously frozen poultry. Workshop on Hyperspectral Image and Signal Processing, Evolution in Remote Sensing IEEE Computer Society.
- Faustman, C., Q. Sun, R. Mancini, and S. P. Suman. 2010. Myoglobin and lipid oxidation interactions: mechanistic bases and control. *Meat Sci.* 86:86–94.
- Gowen, A. A., C. Esquerre, C. P. O'Donnell, and G. Downey. 2010. Influence of polymer packaging films on hyperspectral imaging data in the visible–near-infrared (450–950 nm) wavelength range. *Appl. Spectrosc.* 64:304–312 304-312 64.
- Grunert, T., R. Stephan, M. Ehling-Schulz, and S. Jöhler. 2016. Fourier transform infrared spectroscopy enables rapid differentiation of fresh and frozen/thawed chicken. *Food Control* 60:361–364.
- Hansen, E., D. Juncher, P. Henckel, A. Karlsson, G. Bertelsen, and L. H. Skibsted. 2004. Oxidative stability of chilled pork chops following long term freeze storage. *Meat Sci.* 68:479–484.
- Hastie, T., R. Tibshirani, and J. Friedman. 2009. *The Elements of Statistical Learning: Data Mining, Inference, and Prediction.* 2nd ed. Springer Science & Business Media, New York City, United States.
- James, G., D. Witten, and T. Hastie. 2013. *An introduction to statistical learning.* Springer, New York City, United States.
- Jeong, J. Y., G. D. Kim, H. S. Yang, and S. T. Joo. 2011. Effect of freeze-thaw cycles on physicochemical properties and color stability of beef semimembranosus muscle. *Food Res. Int.* 44:3222–3228.
- Kotsiantis, S. B. 2013. Decision trees: a recent overview. *Artif. Intell. Rev.* 39:261–283.

- Kruglikov, N. A., I. A. Danilenko, R. F. Muftakhetdinova, E. V. Petrova, and V. I. Grokhovsky. 2019. Spectral characteristics of the meteoritic material after the modeling of thermal and shock metamorphism. Page 020227 in AIP Conference Proceedings. American Institute of Physics Inc.
- Lara, M. A., L. Lleó, B. Diezma-Iglesias, J. M. Roger, and M. Ruiz-Altisent. 2013. Monitoring spinach shelf-life with hyperspectral image through packaging films. *J. Food Eng.* 119:353–361.
- Leygonie, C., T. J. Britz, and L. C. Hoffman. 2012. Impact of freezing and thawing on the quality of meat. *Review. Meat Sci.* 91:93–98.
- Liu, Y., F. E. Barton, B. G. Lyon, W. R. Windham, and C. E. Lyon. 2004. Two-dimensional correlation analysis of visible/near-infrared spectral intensity variations of chicken breasts with various chilled and frozen storages. *J. Agric. Food Chem.* 52:505–510.
- Ma, J., H. Pu, D. W. Sun, W. Gao, J. H. Qu, and K.-Y. Ma. 2015. Application of Vis-NIR hyperspectral imaging in classification between fresh and frozen-thawed pork Longissimus Dorsi muscles. Application d'imagerie hyperspectrale Vis-NIR pour la classification entre des muscles longissimus dorsi de porc frais et congel. *Int. J. Refrig.* 50:10–18.
- Otsu, N. 1979. A threshold selection method from gray-level histograms. *IEEE Trans. Syst. Man. Cybern.* 9:62–66.
- Pal, M., and P. M. Mather. 2003. An assessment of the effectiveness of decision tree methods for land cover classification. *Remote Sens. Environ.* 86:554–565.
- Safavian, S. R., and D. Landgrebe. 1991. A Survey of decision tree classifier methodology. *IEEE Trans. Syst. Man Cybern.* 21:660–674.
- Siripatrawan, U., Y. Makino, Y. Kawagoe, and S. Oshita. 2011. Rapid detection of Escherichia coli contamination in packaged fresh spinach using hyperspectral imaging. *Talanta* 55:276–281.
- Soglia, F., A. K. Silva, L. M. Lião, L. Laghi, and M. Petracci. 2019. Effect of broiler breast abnormality and freezing on meat quality and metabolites assessed by 1 H-NMR spectroscopy. *Poult. Sci.* 98:7139–7150.
- Suman, S. P., and P. Joseph. 2013. Myoglobin chemistry and meat color. *Annu. Rev. Food Sci. Technol.* 4:79–99.
- Taghizadeh, M., A. Gowen, P. Ward, and P. O'donnell. 2010. Use of hyperspectral imaging for evaluation of the shelf-life of fresh white button mushrooms (*Agaricus bisporus*) stored in different packaging films. *Innov. Food Sci. Emerg. Technol.* 11:423–431.
- Tang, J., C. Faustman, and T. A. Hoagland. 2004. Krzywicki revisited: equations for spectrophotometric determination of myoglobin redox forms in aqueous meat extracts. *J. Food Sci.* 69:C717–C720.
- Vieira, C., M. T. Diaz, B. Martínez, and M. D. García-Cachán. 2009. Effect of frozen storage conditions (temperature and length of storage) on microbiological and sensory quality of rustic crossbred beef at different states of ageing. *Meat Sci.* 83:398–404.
- Washburn, K. E., S. K. Stormo, M. H. Skjelvareid, and K. Heia. 2017. Non-invasive assessment of packaged cod freeze-thaw history by hyperspectral imaging. *J. Food Eng.* 205:64–73.
- Zulhaidi, H., M. Shafri, A. Suhaili, and S. Mansor. 2007. The performance of maximum likelihood, spectral angle mapper, neural network and decision tree classifiers in hyperspectral image analysis. *J. Comput. Sci.* 3:419–423.